Micro pore throat displacement characteristics of natural gas flooding based on NMR

Changhua Yang[a,b,*], Wei Chen[c], Zhengmao Yang[d], Yang Liu[c], Chunyu Zhao[c], Panpan Lu[a], Min Xu[a]

[a]Petroleum Engineering Institute, Xi'an Shiyou University, Xi'an 710065, China, email: yangch2022@126.com (C. Yang)
[b]Engineering Research Center of Development and Management for Low to Ultra-Low Permeability Oil & Gas Reservoirs in West China, Ministry of Education, Xi'an 710065, China
[c]The No. 11 Oil Production Plant, Changqing Oilfield Branch, Qingyang 745000, China
[d]Exploration and Development Management Department, Sinopec East China oil & Gas Branch, Nanjing 210011, China

ABSTRACT

In order to study the application scope of different gas drive development methods in the micro and nano scale of pore throat, based on the high temperature and high pressure NMR (nuclear magnetic resonance) technology, compared and analyzed the displacement effect of different flooding modes (water drive, natural gas drive and natural bubble gas drive), the pore throat area and the range of throat passage that can be entered by different displacing media, and the contribution rate of different pores to the recovery degree. The experiment shows that the minimum pore throat for water drive is 0.1 μm, and the available pore throat of natural gas drive is two orders of magnitude smaller than that of water drive (0.002–0.01 μm). The pore throat driven by natural gas bubble is 1 orders of magnitude smaller than that of the water drive. The remaining oil is mainly distributed in small pores with uniform distribution.

Keywords: Natural gas; NMR; Natural gas flooding; Foam flooding

1. Introduction

In recent years, natural gas flooding technology has developed rapidly at home and abroad, which is an important development technology after water flooding and polymer flooding. Natural gas flooding is relatively abundant and can be recycled, which is convenient for large-scale application [1–3]. In addition, it does not damage the formation and is not corrosive. This technology has achieved good results in various countries [4]. The methods of using natural gas (hydrocarbon) to improve recovery include natural gas stimulation [5], natural gas flooding [6], etc. With the continuous development of natural gas flooding, the application scope is expanding [7]. From medium and high permeability and low permeability reservoirs to ultra-low permeability and tight reservoirs, the types of gas injection Wells are gradually shifting from straight Wells to horizontal Wells, and at the same time, the production mode is also shifting from gas injection flooding to gas injection huff and puff [8–10].

Study abroad since the 1950s to eighty s began [11], our oil, natural gas flooding development starts late [12], but in recent years have rapid development. So far, more than existing domestic oilfield conducted research and field test of gas flooding, part of the oil block gas flooding also obtain good result [13]. However, the contribution rate of different pores to the recovery degree is not clear and no research has

* Corresponding author.

been carried out on the pore and throat ranges that can be accessed and the producing throat ranges and producing degrees under different natural gas displacement modes.

In recent years, high temperature and high pressure NUCLEAR magnetic resonance technology has developed continuously [14,15], providing a platform for the study of microscopic pore-throat displacement characteristics of natural gas flooding. In this paper, the microscopic pore-throat displacement characteristics of natural gas flooding are studied based on nuclear magnetic resonance technology, which provides a basis for reservoir selection and scheme design of natural gas flooding.

2. Experimental method and basic parameter calibration of NMR

2.1. Experimental methods

The experiment was mainly composed of high temperature and high pressure on-line NMR instrument, thermostat, non-magnetic core gripper, ISCO constant speed and constant pressure pump, intermediate vessel, vacuum pump, pressure gauge, measuring cylinder and so on.

- Core drying process: sample drying for 24 h, temperature (105°C), dry weight. Dry samples were put into NMR equipment to test the basal signal of dry samples.
- Manganese chloride water flooding process: the core is put into the gripper, and manganese chloride water is used to drive, saturated with water.
- Core oil saturation process: one end is used to displace saturated oil, and the other end is left standing for a time (aging) after the end of saturated oil to test T2 spectrum and nuclear magnetic images in saturated oil state.
- Core water flooding process: manganese chloride water was injected at a constant flow rate of 0.2 mL/min. During the experiment, oil and water production was tested until oil was no longer produced. Five different nodes (0.2, 0.5, 1.0, 5 and 10 PV) were injected into the T2 NMR spectrum and image test.
- Core gas flooding process: the outlet end is connected to the gas source, and the gas is injected at constant pressure until the T2 spectrum semaphore basically does not change. T2 and images are tested in the experimental process.
- Core foam flooding process: the core is first injected with 0.2 PV surfactant slug (configured with heavy water), and then gas is injected at constant pressure. The surfactant and gas are mixed at the core injection end to form foam flooding, and the displacement occurs until the T2 spectrum semaphore basically does not change. T2 and images are tested in the experimental process.
- Oil displacement efficiency changes and oil production in pores in gas flooding process are calculated according to spectral line changes [16,17].

2.2. Detection parameters

T2 sampling is CPMG sequence:

Intrinsic parameters: SF = 21 MHz, O1 = 238,590.2 Hz, P1 = 5.6 us, P2 = 12.8 us.

Adjust parameters: SW = 200 KHz, TW = 5,000 ms, RFD = 0.08 ms, RG1 = 20.

DRG1 = 3, NS = 16, DR = 1, PRG = 1, NECH = 8,000, TE = 0.10 ms.

2.3. Porosity calibration and test results

It can be seen from Fig. 1 and Table 1 that the NMR porosity of the selected 67# core is basically the same as that of the weighing method, both of which are about 16%.

3. Experimental results and analysis

3.1. Water drive process

Fig. 2 shows that in the process of water flooding, the spectral line gradually decreases, indicating that the oil in the core is gradually displaced from the core. In the initial stage of water flooding, the oil displacement efficiency varies greatly, and the oil in the larger pore size is mainly displaced from the core.

Fig. 3 shows that in the process of water flooding, the oil displacement efficiency increases gradually. After 5 PV of water flooding, the oil displacement efficiency changes little, and the final oil displacement efficiency of water flooding is 33.34%.

3.2. Natural gas flooding process

Fig. 4 shows that after core water flooding at 10 PV, gas flooding is adopted. In the process of gas flooding, the
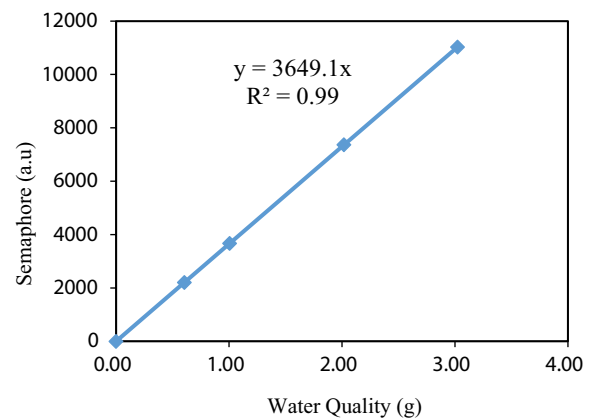
Fig. 1. Porosity sample marking line.

Table 1
Nuclear magnetic porosity measurement results of core samples

Number	67#
Saturated water semaphore (a.u.)	15,616.602
Dry sample semaphore (a.u.)	653.963
Converted water mass (g)	4.10
Diameter (mm)	25.35
Length	51.59
Nuclear magnetic porosity (%)	15.75
Weighing porosity (%)	16.57

spectral line gradually decreases, indicating that oil in core is gradually displaced from core. In the initial stage, the oil in the large pores is driven out of the core, and in the later stage, some oil in the small pores is driven out of the core.
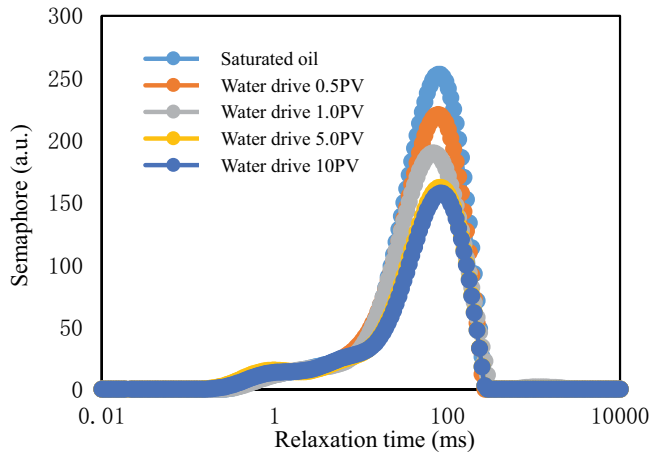
Fig. 2. T2 spectrum of water flooding process.
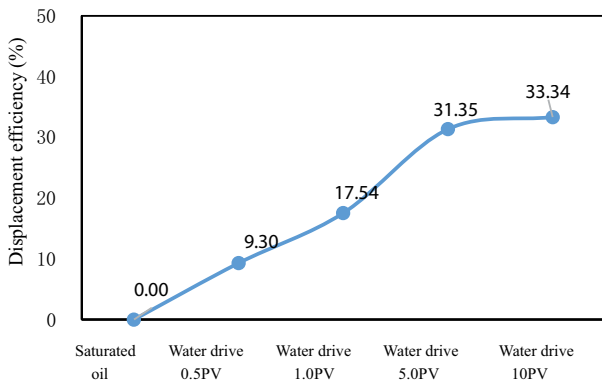
Fig. 3. Oil displacement efficiency of water flooding.
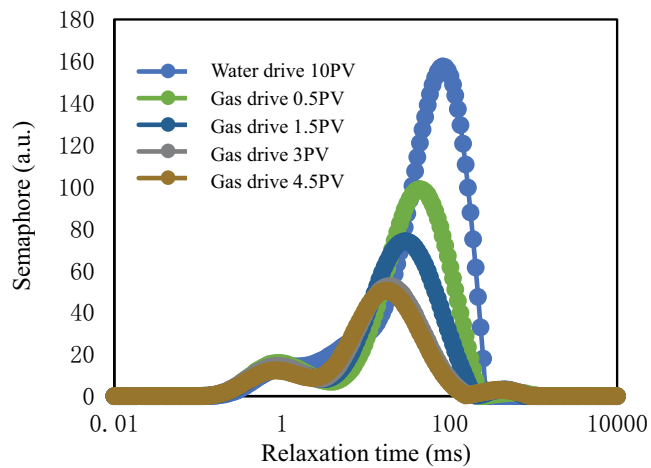
Fig. 4. T2 spectrum of natural gas flooding process.

Fig. 5 shows that in the process of gas flooding, the oil displacement efficiency increases gradually, and after 60 min of gas flooding, the oil displacement efficiency changes little, and the final oil displacement efficiency of 4.5 PV gas flooding is 74.66%. Oil displacement efficiency increased by 41.2% in gas flooding process.

3.3. Natural gas foam flooding

Figs. 6 and 7 show that after gas flooding, foam flooding began. During the process of foam flooding, the spectral line decreased gradually, but the decrease was not large. During foam flooding, the oil displacement efficiency increases gradually, and the oil displacement efficiency is 78.01% after 120 min of foam flooding. The displacement efficiency of foam flooding process increased by 3.35%. Compared with gas flooding, the increase is small, probably because most of the oil in the core has been displaced from the core, and the recovery rate of foam flooding is not obvious.

3.4. Utilization degree of different pore throat interval of natural gas flooding and its contribution to recovery degree

The final recovery factor of core is 78.01%, as shown in Table 2. The contribution degree of water flooding in
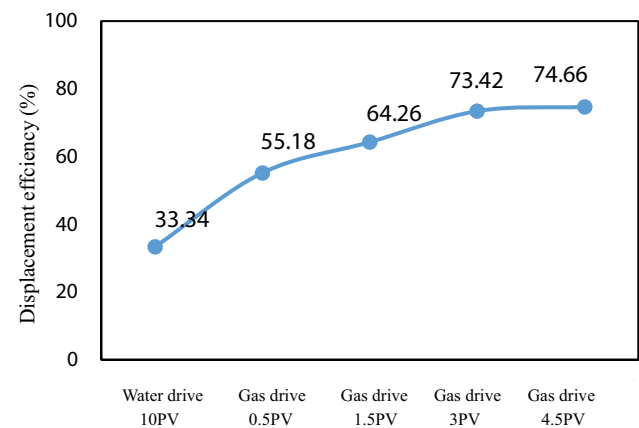
Fig. 5. Oil displacement efficiency of natural gas flooding.
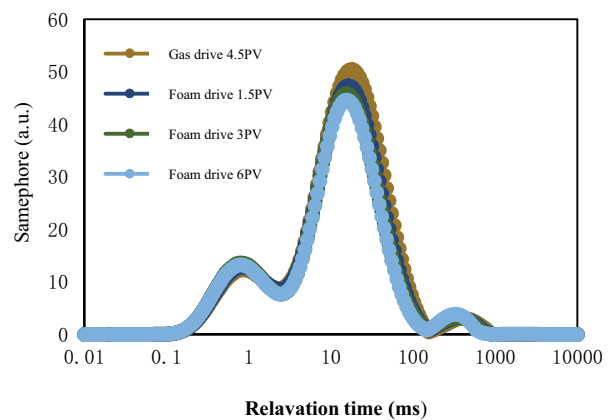
Fig. 6. T2 spectrum of natural gas foam flooding process.

Table 2
The contribution of different pores to recovery

Displacement state	Roar radius < 0.01 μm	Roar radius 0.01–0.1 μm	Roar radius 0.1–2 μm	Roar radius > 2 μm	Final recovery degree (%)
Water drive 10 PV	−1.47	−5.45	20.35	19.91	
Gas drive 4.5 PV	1.07	19.38	14.56	6.31	78.01
Foam drive 6 PV	−1.11	0.41	3.87	0.18	
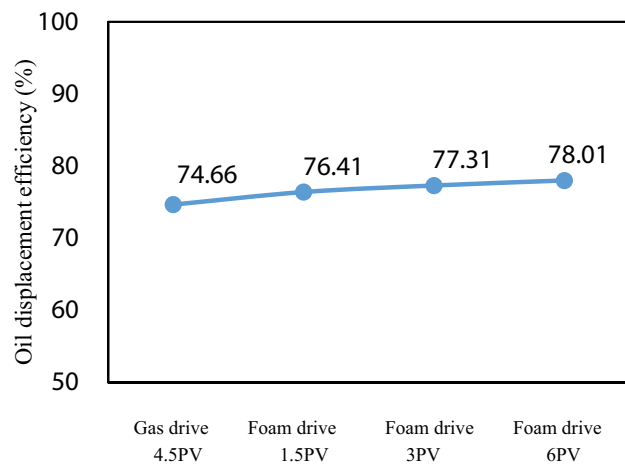
Fig. 7. Oil displacement efficiency of natural gas foam flooding.

Fig. 8. Utilization degree of different pores and throats in natural gas system flooding.
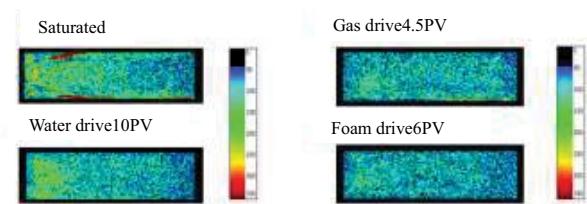
Fig. 9. NUCLEAR magnetic imaging of natural gas displacement process.

different roar is −1.47%, −5.45%, 20.35%, 19.91%, and the overall contribution rate is 33.34%. The contribution degree of gas drive in different roar is 1.07%, 19.38%, 14.56%, 6.31%, and the overall contribution rate is 41.32%. The contribution degree of foam flooding in different roar is −1.11%, 0.41%, 3.87%, 0.18%, and the overall contribution rate is 3.35%. The contribution of water and foam flooding is negative in the micro-gap, mainly because the throat is too small for water and foam to enter and displaces oil from the large pore into the micro-pore, resulting in reduced recovery.

Fig. 8 shows that the maximum pore throat for water drive is 0.1 μm, the available pore throat for NATURAL gas drive is 2 orders of magnitude smaller than that for water drive (0.002–0.01 μm), and the pore throat for natural gas foam drive is 1 order of magnitude smaller than that for water drive. The displaced oil is mainly distributed in pores above 0.1 μm, accounting for 83.5%.

3.5. Core displacement process NMR imaging

During the whole displacement process, water flooding enters from the right end of the core and displaces from the left end of the core, as shown in Fig. 9. According to the color bar, areas with higher oil content are shown in red and areas with lower oil content are shown in blue. It can be observed from the image that the oil in the core gradually decreases, in which the change of water and gas drive stage is more obvious, and the change of foam drive stage is less. The final oil is mainly remaining in small pores with relatively uniform distribution and no obvious remaining oil enrichment area.

4. Conclusion

- HHP NMR study shows that the maximum pore throat for water drive is 0.1 μm, the available pore throat for natural gas drive is two orders of magnitude smaller than that for water drive (0.002–0.01 μm), and the pore throat for natural gas foam drive is one order of magnitude smaller than that for water drive; The displaced oil is mainly distributed in pores above 0.1 μm.
- The contribution rate of water flooding is greater than 0.1 μm in the radius of roar, and the contribution rate of gas flooding and foam flooding is greater in the radius of roar between 0.01 and 2 μm.
- NMR images show that the oil in the core decreases gradually, and the change is more obvious in water and gas flooding stage, but less in foam flooding stage. The final oil is mainly remaining in small pores with relatively uniform distribution and no obvious remaining oil enrichment area.

References

[1] J.-C. Feng, Y. Wang, X.-S. Li, G. Li, Y. Zhang, Z.-Y. Chen, Effect of horizontal and vertical well patterns on methane hydrate dissociation behaviors in pilot-scale hydrate simulator, Appl. Energy, 145 (2015) 69–79.

[2] S.T. Lu, Feasibility Study on Enhanced Oil Recovery by Natural Gas Flooding in Dongshengpu Buried-Hill Reservoir, Northeast Petroleum University, Daqing, 2014.

[3] M. Zheng, J.Z. Li, X.Z. Wu, S.J. Wang, Q.L. Guo, X.M. Chen, J.D. Yu, Potential of oil and gas resources in major petroliferous basins of China and key exploration areas in the future, Earth Sci., 44 (2019) 833–847.

[4] Y. Yang, Research status of enhanced oil recovery by natural gas injection in tight reservoirs, Petrochem. Technol., 27 (2020) 54+333.

[5] W.L. Guan, S.H. Wu, J. Zhao, X.L. Zhang, J.Z. Liang, X. Ma, Utilizing Natural Gas Huff and Puff to Enhance Production in Heavy Oil Reservoir, International Thermal Operations and Heavy Oil Symposium, Calgary, Alberta, Canada, October 20–23, 2008.

[6] N. Mungan, Canada - World Leader in hydrocarbon miscible flooding, J. Can. Pet. Technol., 41 (2002) 35–37.

[7] T.Y. Zheng, X.G. Liu, Z.M. Yang, Y.T. Luo, Y.P. Zhang, Y. He, S.C. Xiong, Research progress of enhanced oil recovery by natural gas injection in tight reservoirs, Appl. Chem., 49 (2020) 190–195+201.

[8] C.N. Zou, Z. Yang, G.S. Zhang, S.Z. Tao, R.K. Zhu, J.X. Yuan, L.H. Hou, D.Z. Dong, Q.L. Guo, Y. Song, Q.Q. Ran, S.T. Wu, B. Bai, L. Wang, Z.P. Wang, Z.M. Yang, B. Cai, Unconventional petroleum geology establishment and practice, J. Geol., 93 (2019) 12–23.

[9] H.B. Todd, J.G. Evans, Improved Oil Recovery IOR Pilot Projects in the Bakken Formation, Society of Petroleum Engineers, Colorado, USA, 2016.

[10] B.T. Hoffman, Huff-N-Puff Gas Injection Pilot Projects in the Eagle, Society of Petroleum Engineers, Alberta, Canada, 2018.

[11] K.P. Ramachandran, O.N. Gyani, S. Sur, Immiscible Hydrocarbon WAG: Laboratory to Field, SPE Oil and Gas India Conference and Exhibition, Mumbai, India, January 20–22, 2010.

[12] Z.C. Liu, J.R. Hou, Z.H. Gao, Y.L. Wu, The Feasibility Studies of Natural Gas Flooding in Ansai Field, International Petroleum Conference and Exhibition of Mexico, Villahermosa, Mexico, March 3–5, 1998.

[13] S.A. Zhang, J.X. Guo, Research Progress of Enhanced Oil Recovery by Natural Gas Injection, Research Progress in Enhancing Oil Recovery by Natural Gas Injection, 2018.

[14] Y.J. Gong, S.B. Liu, M.J. Zhao, H.B. Xie, K.Y. Liu, Nuclear magnetic resonance (NMR) and high-pressure mercury injection (HHG) were used to characterize pore throat distribution in tight oil reservoir, Exp. Pet. Geol., 38 (2016) 389–393.

[15] H.L. Cheng, L.J. Sun, Y.H. Wang, X.Y. Chen, Effects of actual loading waveforms on the fatigue behaviours of asphalt mixtures, Int. J. Fatigue, 151 (2021) 106386, doi: 10.1016/j.ijfatigue.2021.106386.

[16] H.B. Li, J.Y. Zhu, H.K. Guo, NMR T_2 spectrum conversion method for pore radius distribution, J. Spectrosc., 2 (2008) 273–280.

[17] W. Mao, H.B. Jia, P.J. Du, Application of nuclear magnetic resonance technology in the study of oil-water two-phase seepage characteristics, Special Reservoir, 18 (2011) 103–105+129.